Appearance of de Gennes length in force-induced transitions

Keerti Chauhan,[1] Garima Mishra [ORCID],[2] Vimal Kishore,[1] and Sanjay Kumar[1]

[1]*Department of Physics, Banaras Hindu University, Varanasi 221 005, India*
[2]*Department of Physics, Ashoka University, Sonipat 131 029, India*

Using Langevin dynamic simulations, a simple coarse-grained model of a DNA protein construct is used to study the DNA rupture and the protein unfolding. We identify three distinct states: (i) zipped DNA and collapsed protein, (ii) unzipped DNA and stretched protein, and (iii) unzipped DNA and collapsed protein. Here, we find a phase diagram that shows these states depending on the size of the DNA handle and the protein. For a less stable protein, unfolding is solely governed by the size of the linker DNA, whereas if the protein's stability increases, complete unfolding becomes impossible because the rupture force for DNA has reached a saturation regime influenced by the de Gennes length. We show that unfolding occurs via a few intermediate states by monitoring the force-extension curve of the entire protein. We extend our study to a heterogeneous protein system, where similar intermediate states in two systems can lead to different protein unfolding paths.

Single-molecule force spectroscopy (SMFS) is a tool that directly probes structural changes of biomolecules under the influence of external force [1–7]. Since molecular interactions are ubiquitous in biology, insights gathered from SMFS experiments enabled us to understand important cellular mechanisms by which biological systems are able to sense, transduce, and generate mechanical forces *in vivo* [7–13]. In SMFS experiments, usually the biomolecule of interest is attached with a linker (polyproteins or DNA) and pulled from one end with a mechanical spring. From the force-extension ($f - x$) curves, one constructs the free-energy landscape of the biomolecule [14–17]. An inverse Weierstrass transform (IWT) of the Jarzysnki free-energy integral has been used to reconstruct the free energy landscape obtained from single molecule experiments [18–20]. The results obtained are consistent with the weighted histogram method. Hinczewski *et al.* [21] derived a method to calculate the intrinsic free-energy profiles, which account for fluctuations of the DNA handles, rotation of the optical beads, variations in applied tension due to finite trap stiffness, environmental noise, and limited bandwidth of the apparatus. The influence of linkers has also been explored with the assumption that during the stretching, it gives entropic contribution to the free energy [22,23]. It was believed that, in the case of protein, all residues contribute equally to the thermodynamic stability of the protein structure provided by its hydrophobic core. Hence it was expected that the mechanical unfolding of a protein remains insensitive to the structure of the protein and nature of the linker, and depends only on the free energy of the protein, and the transition could in general be described as a two-state (folded-unfolded) process [24–28].

Efforts have also been made to unfold protein using partner-assisted pulling (PAP) and handle-assisted pulling (HAP) [29,30] and revealed substantial variations in the mechanical response of proteins. In PAP mode, protein not only withstands a higher magnitude of force than HAP but also prefers unfolding with the shorter extension of contour lengths. PAP appears to be the combination of the anisotropic response of proteins when simultaneously pulled from spatially distributed multiple points, thus effectively at multiple directions. The anisotropy in the mechanical response of proteins with the pulling geometry and directions appears to play a crucial role in understanding the stability of biopolymers [30]. These studies also suggest that the pulling direction and structure may exhibit multistep transitions corresponding to the energy landscape of several local minima. Therefore, it may be of interest to understand the role of the linker (DNA) in pulling protein, where the structure changes while the free energy remains constant.

Notably, utilizing the ladder model of DNA under the external force, de Gennes showed that the rupture force, $F_c = 2f_1[\chi^{-1} \tanh(\chi \frac{L}{2})]$, of DNA increases linearly with the length (L) of DNA and saturates at some force [31]. Here, f_1 is the force required to separate a single base pair and χ^{-1} is the de Gennes characteristic length [31–36]. The rupture force measured by Danilowicz *et al.* [9] is in excellent agreement with de Gennes's prediction based on the minimal model. However, for a DNA-protein system, it remains a matter of quest whether a linker (DNA) attached to a protein can undergo the force-induced transitions (rupture) before the protein unfolds or not, if one varies the length of the linker.

This Letter aims to explore the influence of de Gennes's length on the unfolding of proteins and identify the role of protein structures in the unfolding mechanism. For this, we construct a minimal coarse grain model of DNA protein construct (DPC) [31,37], where DNA and protein have the ladder and β-sheet structures [31,37] [Fig. 1], respectively. The model is similar to the one used in experimental and theoretical studies to get the free energy landscape of proteins by unfolding it using linker [2,7,22]. Here, we explore the influence of de Gennes length on the unfolding of different β sheet proteins having almost the same energy, which remained elusive.

In the present model, ith nucleotide of one strand of DNA can form a native pair with the ith nucleotide of the
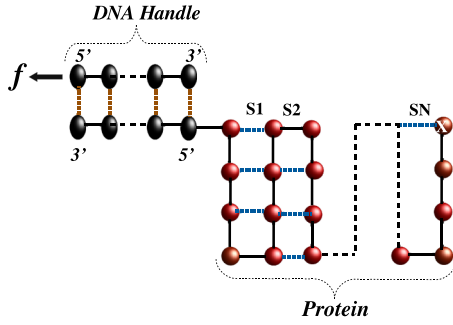
FIG. 1. Schematic diagram of a DNA-protein construct (DPC). Black spheroids represent monomers in DNA and red spheres denote beads in proteins. An external force (f) is applied to the $5'$ end of the DNA strand, whereas the $5'$ of the other strand is linked with a β-sheet protein. The last bead of the protein, shown with a cross mark, is anchored.
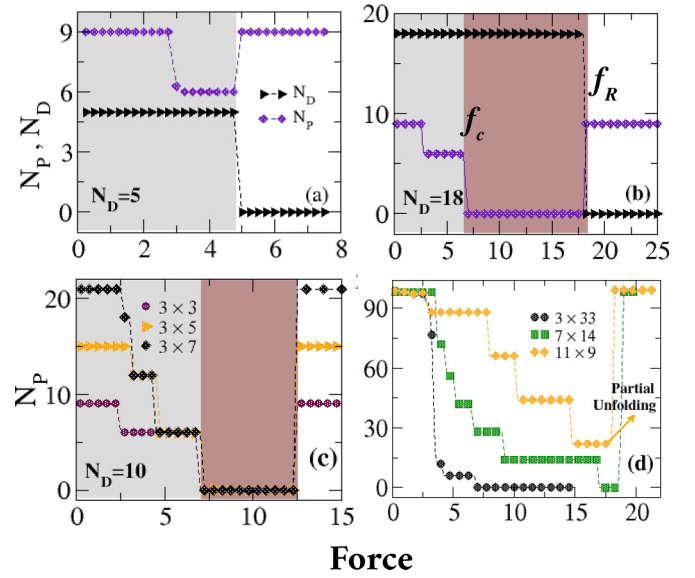

FIG. 2. Variation of the number of intact DNA base pairs N_D and nonbonded native contacts in protein N_p as a function of force f for a fixed size protein ($m \times N$) linked to variable lengths of DNA (N_D): (a) 3×3 β-sheet protein, $N_D = 5$, where $f_R \ll f_C$, (b) 3×3, $N_D = 18$, $f_R \gg f_C$, (c) $N_D = 10$, $f_R > f_C$, and (d) $N_D = 18$, where $f_R \gg f_C$ for different m, while keeping ($m \times N$) or energy of the system almost constant.

complementary strand of DNA [31,38]. The protein is composed of N number of sheets (labeled as S1 to SN), where each sheet has m number of nonbonded native contacts [Fig. 1(a)]. The native pairs in both DNA and protein interact via Lennard Jones potentials, whereas the backbone beads are attached with a harmonic spring. Since the strengths of hydrogen bonds are different in protein and DNA [39–41], therefore, we consider different strengths for hydrogen bond interactions for protein ($A_{i,j} = 1.5$) and DNA ($A_{i,j} = 1.0$) in Eqs. SM2 and SM3 [42], respectively. The time evolution of the system is studied using Langevin dynamics simulations [43–45]. More detailed exposition can be seen in the Supplemental Material [42]. Under the applied force, an isolated protein can either be in (i) collapsed or folded [P(C)] state or (ii) stretched or unfolded [P(S)] state at any temperature $T < T_C$, where T_C is the unfolding temperature. In the stretched state, all the native contacts in protein (N_P) are broken. The force required for complete unfolding is called the critical force (f_C) below which protein remains in the folded state (including partially unfolded states). Similarly for the isolated DNA having N_D base pairs, we define a rupture force (f_R) below which a DNA is in the zipped state [D(Z)] and above it in the unzipped state [D(U)], where all the base pairs get dissociated ($N_D = 0$) with each other. For the DPC, we first study the response of the applied force on the number of intact bonds N_P and N_D for a 3×3 β-sheet protein attached with a DNA handle of different lengths. For a handle of small size, e.g., $N_D = 5$ [Fig. 2(a)], f_c is larger than f_R indicating that the DNA ruptures at a lower force and the protein remains in the folded state. Protein gets unfolded once the size of the handle exceeds a particular length (see Fig. SM 2 [42]). If the size of the DNA handle becomes large enough, e.g., $N_D \geqslant 18$ [Fig. 2(b)], protein unfolds under the applied force ($f_C \sim 7.5$) and stays in the stretched states. At $f = f_R$, the DNA ruptures and the protein refolds to its native state.

Next, we set the length of the DNA constant ($N_D = 10$) and vary the number of sheets (N) in the protein [Fig. 1] keeping m fixed. Interestingly, here all the proteins (with $m = 3$) of different N unfold at the same critical force $f = f_c \approx 7.5$ followed by DNA ruptures at $f_R = 12.5$ [Fig. 2(c)]. This indicates that, for the β sheet, the complete unfolding is governed

by the local opening of the m nonbonded contacts and remains independent of the number of sheets. However, the number of intermediate steps in which protein unfolds increases with increasing N. The number of these intermediate steps (1 for $N = 3$, 2 for $N = 5$, and 3 for $N = 7$) and the corresponding values of N_P indicate sheets unfold in pairs but only after the opening of the first sheet (smaller first step size). It shows the influence of the protein structure (β sheet) in the force-induced transition. Also, for large N, say $N = 33$ in Fig. 2(d), the existence of an effective single-step protein unfolding is consistent with the observation made in [46].

To have a deeper insight into the mechanism involved in the DPC, we look at the unfolding of different configurations of protein ($m \times N = N_P \approx 99$) for a fixed length of DNA handle ($N_D = 18$). The response of the applied force on the DPC is shown in Fig. 2(d) and Fig. SM 3 [42]. It is evident that protein structures with larger m have better stability of the protein, irrespective of the N value. For a 3×33 protein ($m = 3$, $N = 33$), complete unfolding takes place at $f_C \approx 7.5$, whereas for $m = 7$ ($N = 14$), $f_C = 17.25$, to unfold protein (Fig. SM 3 [42]). It is important to note that while f_C increases with m, f_R reaches its saturation value ~ 20 [33], which implies that, after a certain value of m, DNA (for any N_D) will always rupture before the complete unfolding of the protein. Consequently, one cannot observe the complete unfolding of the protein at higher values $m \geqslant 8$ such as 11×9 protein unfolds partially (Fig. SM 3 [42]).

The phase diagram shown in Fig. 3 summarizes the combined response of f, N_D, and $N_P(m \times N)$. The phase boundary represented by a solid line with square markers separates zipped DNA and the collapsed protein [D(Z) + P(C)] state from the zipped DNA and stretched or unfolded protein
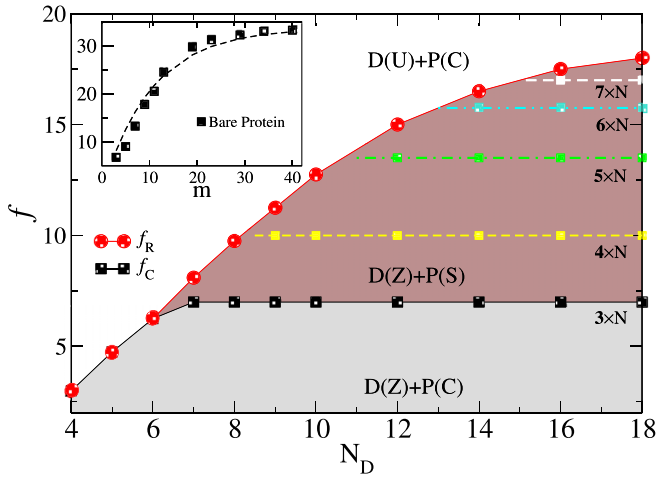
FIG. 3. Phase diagram showing different states of the DPC for different force values. The f_R line separates the zipped (Z) from the unzipped (U) DNA phase and f_C separates between collapsed (C) and stretched (S) protein states. In the inset, we have plotted f_C vs m for a bare protein, where the square shows the results obtained from the simulation up to $40 \times N$ protein and the dotted line shows the analytical result proposed for DNA unzipping (see Supplemental Material [42]).

[D(Z) + P(S)]. The solid line with circles separate the unzipped DNA and collapsed protein [D(U) + P(C)] state with other states i.e. [D(Z) + P(S)] or [D(Z) + P(C)]. Now, we put our emphasis on the phase diagram of $3 \times N$ protein, where a DNA handle of variable length has been used to probe the stability of DPCs. In Fig. 3, the line having solid red circles represents the rupture force f_R as a function of N_D. The rupture force first increases with the N_D and later shows saturation. The line with solid black squares shows the critical force f_C of the unfolding of a $3 \times N$ β-sheet protein. For small lengths of DNA handle ($N_D < 7$), f_R is smaller than f_C. As a result, we observed a transition from the D(Z)+ P(C) state to the D(U) + P(C) state. This implies that the protein remains intact (or partially unfolded) during this transition. When the length of the DNA handle exceeds $N_D \geqslant 7$, the DPC shows the transition from the D(Z)+ P(C) state to the D(Z) + P(S) state. This is due to the fact that a large DNA handle can sustain more force and remains in the zipped state at higher forces, whereas the force required to unfold the protein f_C still remains the same. As a result, the protein unfolds first before the DNA rupture. If we further increase the force, the system shows a second transition from the D(Z) + P(S) state to the D(U) + P(C) state indicating that the protein refolds back after the rupture of DNA.

The observation that f_c increases with increasing (m) [Fig. 2(d)] is represented using broken lines ($3 \times N, 4 \times N, \ldots, 7 \times N$) in Fig. 3. As a consequence the D(Z)+P(S) region shrinks in the phase diagram and, for a large m, the D(Z)+P(S) state does not appear anymore. For $f_c > f_R$, DNA rupture occurs prior to the protein achieving full unfolding and prohibits the occurrence of simultaneous rupture of DNA and unfolding of protein [47]. Thus we conjecture that a protein having β-sheet structure cannot be unfolded for arbitrary larger m (in this case $m \geqslant 7$). One can note that though the

unfolding force increases with m, it also shows saturation like DNA.

The physical origin for such saturation is attributed to the presence of de Gennes's length in the DNA. It would be intriguing to investigate whether a similar characteristic length exists in the β-sheet protein. We plotted f_C as a function of m for a bare protein (without DNA handle) in the inset of Fig. 3. Initially f_C increases with m and saturates for the larger values of m resembling the behavior observed in DNA. Notably, the peeling of β-sheet protein is akin to DNA unzipping. Following Ref. [35], we used an extended ladder model for DNA unzipping to fit the f_C for a bare protein. The dashed line, obtained from Eq. SM 8, remarkably matches the simulation results. It suggests the presence of a length scale in the β-sheet protein, similar to the de Gennes length seen in DNA, which may alter the response of the force on DPC.

We now investigate the role of β-sheet structure of a protein by looking at the force-extension curves [in Fig. 4(a)] for the $3 \times N$ DPC during unfolding. Notably, distinct plateaus in the $f - x$ curves reveal the opening of various sheets, resembling the unfolding pattern observed in titin [1]. At smaller forces $f < f_C$, each plateau in the $f - x$ curves provides information about an individual sheet opening that gives a fixed extension over the range of the force (Fig. SM 4) [42,48]. At a very high force $f \geqslant f_C$, all the protein sheets are open. Once f reaches the value of the rupture force ($f \geqslant f_R$), DNA ruptures, and protein refolds to its native state. Snapshots of the unfolding of protein corresponding to different steps in the $f - x$ curve are shown in Fig. SM 5 [42].

We also calculate the probability of opening of the sheets Si contributing to these plateaus in Figs. 4(b)–4(d). This has been illustrated using a color map for a range of proteins, each characterized by distinct N. Yellow indicates the unfolded sheet, while blue represents the folded sheets. Other colors in between reflect mixed probabilities during unfolding. Though we have applied the force through the DNA handle on the β sheet protein, which is connected to only the end of the S1 sheet, the anchored end of the SN sheet also experiences an equal and opposite force. As expected, one can see the opening of either the S1 or SN sheet contributing to the first observed plateau. However, one can also note that the opening of S1 is quite frequent compared to SN at low forces (see Fig. SM 4 for details [42]). In fact, the probability P(S1) of having sheet S1 in an unfolded state always dominate over the P(SN) as f increases. This is because the end monomer of the SN sheet is fixed; therefore, the entropic contribution arising due to the anchored end is less compared to the end attached to the DNA handle, although the applied force contribution remains the same at both ends. This asymmetry in the unfolding becomes more apparent in the proteins having five sheets [Fig. 4(c)] and seven sheets [Fig. 4(d)]. We expect this asymmetry to disappear if we pull the protein using both of the ends (similar to the dual beam optical tweezer setup), as the entropic force will work on both ends of the protein. Therefore, one expects a symmetric unfolding of the protein. At intermediate forces ($2.5 < f < f_C$), we note the unfolding of more than one sheet corresponding to observed plateaus in the $f - x$ curve [Fig. 4(a)]. In this force range, the opening of the next sheet will depend upon the already unfolded sheets. It happens due to the stochastic force which
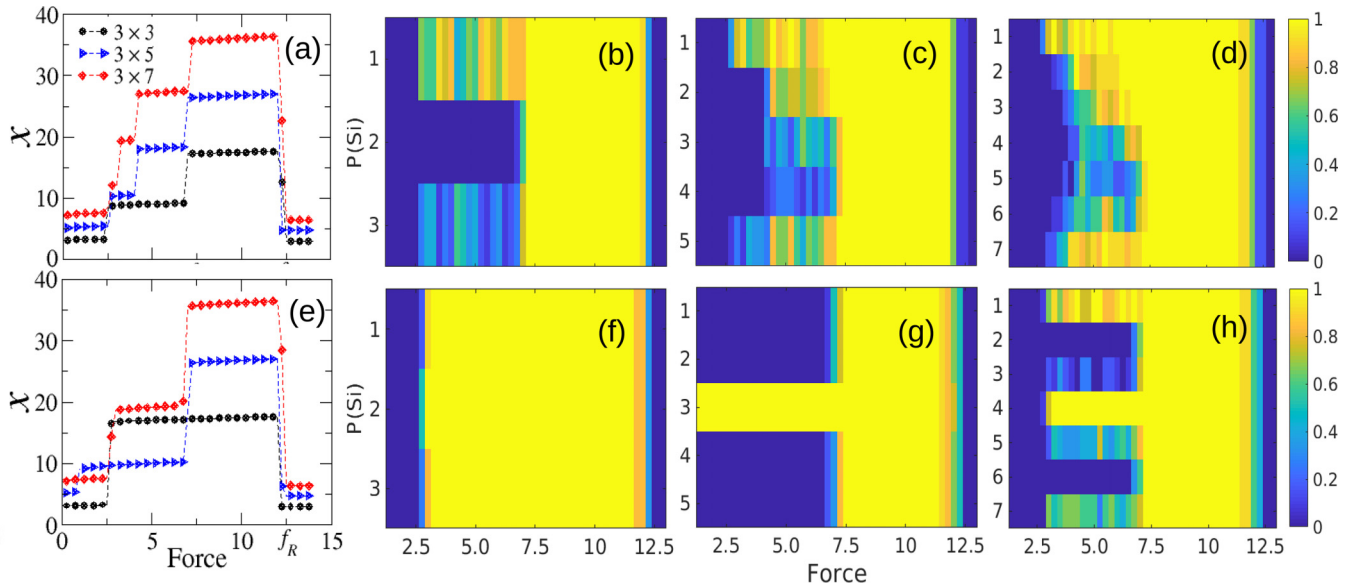
FIG. 4. (a) $f - x$ diagram for the homogeneous protein; [(b)–(d)] color map showing the probability of opening of an individual sheet (SM) as a function of the applied force f for (b) 3×3, (c) 3×5, and (d) 3×7 protein. (e) $f - x$ diagram for the heterogeneous (central weak) protein; [(f)–(h)] color map showing the probability of opening of an individual sheet as a function of the applied force f for (f) 3×3, (g) 3×5, and (h) 3×7 protein having weaker central sheets.

acts more prominently at the newly exposed free ends. It is also worth mentioning that the intermediate sheets get unfolded in pairs as evident in Figs. 4(c) and 4(d). Importantly, the central sheets remain in the folded state up to the applied force ≈7.5. With the unfolding of central sheets at the critical force, the protein acquires the stretched state. Once, all the sheets are in an unfolded state, the further increase in the force ($7.5 < f < 12.5$) contributes towards the stretching of covalent bonds between consecutive monomers until the applied force becomes strong enough to rupture the DNA (e.g., $f_R = 12.5$ for $N_D = 12$). As DNA ruptures at $f = f_R$, the protein refolds to its native state as seen in Figs. 4(a)–4(d). It is pertinent to note that the refolding of all the sheets happens at the same rupture force $f_R = 12.5$.

Current understanding highlights that the structure and stability of a protein strongly depend on the arrangements and compositions of the hydrophilic and hydrophobic residues. The hydrophobic residues tend to occupy the protein's interior (core), whereas hydrophilic residues prefer the protein's surface [49–52]. It is also reported that the water-mediated interaction destabilizes the core of proteins [53–55] and helps the unfolding. Notably, for the mechanical unfolding of a wild-type I27 concatemer with that of (I27)(5)*, the observed forces are considerably lower and the core destabilization has little effect on the unfolding [29,56,57].

Considering the higher stability of the middle sheet during unfolding [Figs. 4(a)–4(d)], we reduce its interaction strength. This affects the mechanical stability of the modeled protein. We use a $3 \times N$ DPC setup with decreased attractive interaction among native nonbonded contacts in the central sheet. This is done by lowering the nearest neighbor interaction ($A_{i,j}$) of the middle sheet, from 1.5 to 1.0 (Fig. SM 6 [42]). We show the corresponding $f - x$ curve for this mixed system in Fig. 4(e). Again, unfolding occurs in steps as force increases: instant refolding followed by DNA rupture. However, opening

pathways differ from the homogeneous protein [Fig. 4(a)]. The number of plateaus is reduced as we see a single-step opening for $N = 3$ and a two-step opening for $N = 5$ and $N = 7$ [Fig. 4(e), SM 7 [42]]. Unfolding probability for sheets is shown in Figs. 4(f)–4(h). At $f \approx 2.5$, the middle sheet unfolds first, contrary to prior stability in the homogeneous case. In 3×3, all sheets unfold at $f \approx 2.5$; the middle sheet's unfolding prompts other sheets [Figs. 4(e) and 4(f) and SM 7a [42]] to unfold. For the 3×5 protein [Figs. 4(g) and SM 7b [42]], the central weaker sheet opens at $f < 2.5$, forming compact globules (S1+S2 and S4+S5). These globules keep on resisting the unfolding until $f \approx f_C$. At $f \approx 7.5$, all other sheets open, reaffirming paired intermediate sheet unfolding. In the 3×7 protein, despite S4's weakness, S1 or S7 can unfold with S4 at lower force ($f \approx 2.5$). Among these, the weakest sheet has the highest opening probability [Fig. 4(h)]. Variations in 3×5 and 3×7 proteins may arise from covalent bond positions; 3×5's bond differs from 3×3 and 3×7 (Fig. SM 6 [42]). Probabilities in Fig. 4(h) stem from competing opening mechanisms, tied to the first opening sheet's identity. If S4 opens first, DPC shifts to two 3×3-like globules, showing pattern akin to the homogeneous 3×3 protein's higher force opening. Entropic asymmetry leads to S1-side opening dominance over the SN end. For $f < 7.5$, middle sheets (S2 and S6) stay stable in two globules until both unfold at $f \approx 7.5$, rendering the entire protein unfolded.

In summary, we examined the DNA-protein composite phase diagram under the external force, exploring the DNA rupture together with protein unfolding. Although the model ignores the microscopic details such as non-native interactions, inter- and intrastrand interactions, persistence length of DNA, etc., the phase diagram obtained here provides very rich behaviors. Here, the native interaction among the nonbonded nearest neighbor in the β sheet is considered higher than the native base pairing interaction in DNA. We have demonstrated

that the sequence of rupture and unfolding depends on the length of DNA and the number of contacts (m) in the β sheet. However, if the native interaction among nonbonded nearest neighbors and native base pairing interaction in DNA have equal strength, the β sheet always unfolds first, followed by DNA rupture as the force increases.

The plateaus observed in the force-extension curves revealed the presence of intermediate states. The complete unfolding takes place almost at the same force as seen in experiments [56]. The observation that f_c is independent of N is also in agreement with Ref. [46], where the protein CI2, having 80 residues, and another Barnase protein, with 140 residues, unfold at nearly the same critical force.

The key finding is that as the number of contacts per sheet increases, the unfolding force also increases, eventually saturating for higher values of m. This provides support for the presence of a protein length that corresponds to DNA's de Gennes length. Consequently, for m values surpassing a threshold, protein unfolding becomes impossible, as DNA handle rupture occurs prior to protein unfolding.

The probabilistic pathways of the unfolding of protein provide important insights into the unfolding mechanism of a protein. Making the central sheet weaker showed the importance of water solvent (weakens the core region), leading to reduced unfolding force and novel unfolding pathways. The complete phase diagram of DPC presented here calls for new experiments to explore the various phases of DPC, offering deeper insight into DNA-protein interaction in living systems. Additionally, further investigation is warranted to determine whether a length scale similar to the de Gennes length observed in the model system exists in β-sheet proteins.

[1] M. S. Z. Kellermayer, S. B. Smith, H. L. Granzier, and C. Bustamante, Science **276**, 1112 (1997).

[2] K. C. Neuman and A. Nagy, Nat. Methods **5**, 491 (2008).

[3] C. Bustamante, Z. Bryant, and S. B. Smith, Nature (London) **421**, 423 (2003).

[4] S. Kumar and M. S. Li, Phys. Rep. **486**, 1 (2010).

[5] U. Bockelmann, B. Essevaz-Roulet, and F. Heslot, Phys. Rev. Lett. **79**, 4489 (1997).

[6] J. F. Marko and E. D. Siggia, Macromolecules **28**, 8759 (1995).

[7] S. Kumar and G. Mishra, Soft Matter **7**, 4595 (2011).

[8] G. U. Lee, L. A. Chrisey, and R. J. Colton, Science **266**, 771 (1994).

[9] C. Danilowicz *et al.*, Phys. Rev. Lett. **93**, 078101 (2004).

[10] A. Galera-Prat *et al.*, Curr. Opin. Struct. Biol. **20**, 63 (2010).

[11] C. P. Johnson *et al.*, Science **317**, 663 (2007).

[12] J. F. Marko, Chromosome Res. **16**, 469 (2008).

[13] S. B. Smith, Y. Cui, and C. Bustamante, Science **271**, 795 (1996).

[14] Y. Seol, G. M. Skinner, K. Visscher, A. Buhot, and A. Halperin, Phys. Rev. Lett. **98**, 158103 (2007).

[15] C. Ke, M. Humeniuk, H. S-Gracz, and P. E. Marszalek, Phys. Rev. Lett. **99**, 018302 (2007).

[16] F. A. Carvalho, I. C. Martins, and N. C. Santos, Arch. Bioch. Biophys. **531**, 116 (2013).

[17] P.-G. De Gennes, *Scaling Concepts in Polymer Physics* (Cornell University Press, Ithaca, NY, 1979).

[18] G. Hummer and A. Szabo, Proc. Natl. Acad. Sci. USA **107**, 21441 (2010).

[19] M. T. Woodside and S. M. Block, Annu. Rev. Biophys. **43**, 19 (2014).

[20] M. C. Engel, D. B. Ritchie, D. A. N. Foster, K. S. D. Beach, and M. T. Woodside, Phys. Rev. Lett. **113**, 238104 (2014).

[21] M. Hinczewski, C. M. J. Gebhardt, M. Rief, and D. Thirumalai, Proc. Natl. Acad. Sci. USA **110**, 4500 (2013).

[22] V. P. Reddy Chichili, V. Kumar, and J. Sivaraman, Protein Sci. **22**, 153 (2013).

[23] M. Frei, S. V. Aradhya, M. S. Hybertsen, and L. Venkataraman, J. Am. Chem. Soc. **134**, 4003 (2012).

[24] R. Zwanzig, Proc. Natl. Acad. Sci. USA **94**, 148 (1997).

[25] J. Schönfelder, D. De Sancho, R. Berkovich, R. B. Best, V. Muñoz, and R. Perez-Jimenez, Commun. Chem. **1**, 59 (2018).

[26] E. E. Lattman and G. D. Rose, Proc. Natl. Acad. Sci. USA **90**, 439 (1993).

[27] R. Zwanzig, Proc. Natl. Acad. Sci. USA **92**, 9801 (1995).

[28] J. Sabelko, J. Ervin, and M. Gruebele, Proc. Natl. Acad. Sci. USA **96**, 6031 (1999).

[29] D. J. Brockwell, E. Paci, R. C. Zinober, G. S. Beddard, P. D. Olmsted, D. A. Smith, R. N. Perham, and S. E. Radford, Nat. Struct. Mol. Biol. **10**, 731 (2003).

[30] N. Arora, J. P. Hazra, and S. Rakshit, Commun. Biol. **4**, 925 (2021).

[31] P. G. de Gennes, C. R. Acad. Sci., Ser. IV Phys. **2**, 1505 (2001).

[32] M. Mosayebi, A. A. Louis, J. P. Doye, and T. E. Ouldridge, ACS Nano **9**, 11993 (2015).

[33] R. Mishra, T. Modi, D. Giri, and S. Kumar, J. Chem. Phys. **142**, 174910 (2015).

[34] S. Nath, T. Modi, R. Mishra, D. Giri, B. Mandal, and S. Kumar, J. Chem. Phys. **139**, 165101 (2013).

[35] A. Singh, T. Modi, and N. Singh, Phys. Rev. E **94**, 032410 (2016).

[36] A. Singh and N. Singh, Phys. Rev. E **92**, 032703 (2015).

[37] L. Finegold and J. L. Cude, Nature (London) **238**, 38 (1972).

[38] K. Chauhan, A. R. Singh, S. Kumar, and R. Granek, J. Chem. Phys. **156**, 164907 (2022).

[39] Y. Senju, M. Kalimeri, E. V. Koskela, P. Somerharju, H. Zhao, I. Vattulainen, and P. Lappalainen, Proc. Natl. Acad. Sci. USA **114**, E8977 (2017).

[40] F. K. Malik and J.-t. Guo, Proteins: Struct. Funct. Bioinf. **90**, 1303 (2022).

[41] The typical hydrogen bond strength in protein lies in the range of 5–6 kcal/mol [39] as compared to 1–5 kcal/mol in DNA [40].

[42] See Supplemental Material at http://link.aps.org/supplemental/10.1103/PhysRevE.108.L042501 for a detailed description of the model and methodology used to study the DPC construct, which includes the following additional figures: (II) variation in number of bonds as a function of force for various systems, an extension of Fig. 2, (III) force-extension figure for single realization for homo and central weak protein, and (IV) other comprehensive figures.

[43] D. Frenkel and B. Smit, *Understanding Molecular Simulation* (Oxford Science, Oxford, UK, 1987).

[44] K. Chauhan and A. Singh, Phys. Rev. E **105**, 064505 (2022).

[45] T. Pal, K. Chauhan, and S. Kumar, Phys. Rev. E **105**, 044407 (2022).

[46] A. Srivastava and R. Granek, Phys. Rev. Lett. **110**, 138101 (2013).

[47] In this scenario, the DNA ruptures irrespective of its length and the protein remains intact as it experiences the force through the DNA handles only. The partially unfolded protein sheets refold to their native state after rupture of DNA and prohibit the occurrence of simultaneous rupture and unfolding.

[48] One unfolded pair contributes to $2mr_0$ distance to the end-to-end distance, where r_0 represents the equilibrium distance between two adjacent beads of a strand.

[49] H. Dong and J. D. Hartgerink, Biomacromolecules **8**, 617 (2007).

[50] S. Malleshappa Gowder, J. Chatterjee, T. Chaudhuri, and K. Paul, Sci. World J. **2014**, 971258 (2014).

[51] C.-J. Tsai, S. L. Lin, H. J. Wolfson, and R. Nussinov, Protein Sci. **6**, 53 (1997).

[52] N. N. Alexandrov and N. Go, Protein Sci. **3**, 866 (1994).

[53] T. Sumi and H. Imamura, Protein Sci. **30**, 2132 (2021).

[54] G. A. Papoian, J. Ulander, and P. G. Wolynes, J. Am. Chem. Soc. **125**, 9170 (2003).

[55] Y. Levy and J. N. Onuchic, Proc. Natl. Acad. Sci. USA **101**, 3325 (2004).

[56] D. J. Brockwell, G. S. Beddard, J. Clarkson, R. C. Zinober, A. W. Blake, J. Trinick, P. D. Olmsted, D. A. Smith, and S. E. Radford, Biophys. J. **83**, 458 (2002).

[57] S. Kumar and D. Giri, Phys. Rev. Lett. **98**, 048101 (2007).